Copper-Based Compounds for Electrochemical Reduction of Carbon Dioxide

Fan YANG

Pei-lin DENG

You-Jia HAN

Pan Jing

Bao-yu XIA
Key Laboratory of Material Chemistry for Energy Conversion and Storage (Ministry of Education), Hubei Key Laboratory of Material Chemistry and Service Failure, Wuhan National Laboratory for Optoelectronics, School of Chemistry and Chemical Engineering, Huazhong University of Science and Technology (HUST), Wuhan 430074, P.R. China, byxia@hust.edu.cn

Copper-Based Compounds for Electrochemical Reduction of Carbon Dioxide

YANG Fan[a], DENG Pei-lin[a], HAN You-Jia, Jing Pan, XIA Bao-yu*

(*Key Laboratory of Material Chemistry for Energy Conversion and Storage* (*Ministry of Education*),
Hubei Key Laboratory of Material Chemistry and Service Failure, Wuhan National Laboratory for
Optoelectronics, School of Chemistry and Chemical Engineering, Huazhong University of
Science and Technology (*HUST*), *Wuhan* 430074, *P.R. China*)

Abstract: The electrochemical reduction of carbon dioxide (CO_2) to useful chemicals and fuels has attracted enormous interest since the deteriorating global warming and energy shortage problems resulted from ever-increasing CO_2 emission. Designing efficient catalysts is of capital significance to realize the efficient and selective conversion of CO_2. Among various catalysts explored, copper-based compounds have promising potentials with acceptable efficiency for hydrocarbon production. Herein, recent advances on copper-based materials are summarized for electrochemical CO_2 conversion. We intend to include the dimensional structure, different forms (alloy, oxide) and molecular catalysts in copper-based catalysts. Moreover, the reaction mechanisms of CO_2 electroreduction on Cu-based catalysts are emphatically discussed. Finally, potential directions are also proposed for future design of highly efficient Cu-based catalysts to promote the rapid development of CO_2 conversion for sustainable world.

Key words: CO_2 conversion; Cu-based material; electrocatalyst; selectivity; reaction mechanism

CLC Number: O646　　　　　　　　　　　**Document Code:** A

With the rapid evolution of global population and industrial revolution, the main contributors of greenhouse gases, CO_2 production and emission, are becoming more thought provoking for energy issues and environmental complications. Except the physical storage strategy, the CO_2 electroreduction can help reduce the level in the atmosphere, and simultaneously produce valuable chemicals and fuels, thus, holding great potentials to solve for these symbiotic issues[1-5]. Among various CO_2 exploitation technologies, electrochemical conversion of CO_2 exhibits the largest potential in developing sustainable future owing to the employment of renewable electric power (solar, wind energy, etc.) and its easily controlled process by external bias (i.e., overpotential) under ambient temperature and pressure[6].

CO_2 electroreduction reaction (CO_2RR) is a complex process involving multiple electrons and pro-tons, and one of the most obvious features for CO_2RR is the catalyst-dependent product selectivity. Various electrocatalysts are developed to realize the selective and efficient conversion of CO_2. Typically, Au, Ag, Zn are active materials for selective production of CO[7-9], some other materials such as Sn, Bi and Pb exhibit a higher selectivity for formate production[10-12]. While Cu-based materials are the only catalyst having efficient ability for hydrocarbon production[13-15], thus, holding the most promising potential for efficiently catalyzing CO_2 to useful fuels and chemicals.

Herein, we focus on the electrochemical CO_2 conversion in the aspects of reaction mechanisms and structure-function relationship based on various Cu-based catalysts. Firstly, the mechanisms of Cu-based materials for CO_2RR are introduced and the hydrocarbon production in the multi-electron transfer process over Cu-based materials is highlighted, and

followed by the relationship discussion between the Cu compound structure and CO_2 electroreduction performance. Finally, challenges and directions of CO_2RR in future development of Cu-based catalysts are summarized and presented to promote the rapid development of this emerging technology. We hope this review paper could provide some useful concepts in designing efficient Cu based electrode for selective CO_2 conversion in future development of sustainable society.

1　Reaction Mechanisms of CO_2 Reduction

Primarily, CO_2 molecular is thermochemically stable due to its linear molecular structure, where C is an electrophilic and O atom belongs to weak Lewis bases. To active and break the O=C bond, a high potential of -1.9 V vs. RHE is needed for the first electron transfer step in the reduction process, CO_2 to CO_2^*. Furthermore, CO_2 electroreduction is a multielectron transfer process, which would result in the diversity of reduction products. Finally, the hydrogen evolution reaction (HER) always competes with CO_2RR in the aqueous solution, which further inhibits the efficiency of CO_2RR. Thus, proper adsorption between catalyst and reaction intermediates is of vital importance for improving the reaction kinetics and product selectivity. The cooperation of theoretical analyses and experimental results are, therefore, absolutely essential to design highly efficient and robust catalysts for real-world application. Generally, the reduction products of 2-electron transfer are CO and HCOOH, while 4, 6, 8 electrons transferred products are HCHO, CH_3OH and CH_4, respectively. Moreover, other hydrocarbons such as C_2H_4 and CH_3CH_2OH are produced by the transfer of 12 electrons. CO_2 electroreduction is a cathodic reaction accompanying with a multiple proton-electron process. Tab. 1 shows the equilibrium potentials for different products[3]. Most of the equilibrium potentials are very close to hydrogen evolution, so the formation of byproduct H_2 is unavoidable. It is difficult to achieve a real high product activity and selectivity for valuable carbon contained products.

Tab.1　Standard hydrogen potential for CO_2 electroreduction

Half reaction of CO_2 reduction	E/V(vs. SHE)
$CO_2 + 2H^+ + 2e \rightarrow CO + H_2O$	-0.53
$CO_2 + 2H^+ + 2e \rightarrow HCOOH$	-0.61
$CO_2 + 4H^+ + 4e \rightarrow HCHO + H_2O$	-0.48
$CO_2 + 8H^+ + 8e \rightarrow CH_4 + 2H_2O$	-0.24
$2CO_2 + 12H^+ + 12e \rightarrow C_2H_4 + 4H_2O$	-0.33
$CO_2 + 6H^+ + 6e \rightarrow CH_3OH + H_2O$	-0.38
$CO_2 + e \rightarrow CO^-$	-1.9
$2H^+ + 2e \rightarrow H_2$	-0.41

Recently, several reaction pathways and possible mechanisms are proposed for CO_2RR based on the experimental and theoretical studies. Hori et al. discussed the distribution of reduction products on Cu electrode under the diverse applied potentials[16]. Initially, with the less negative potentials, the faradaic efficiency (FE) values of CO and HCOOH were increased simultaneously, while the FE of H_2 was dropped at the same time. Thereafter, the FEs of CO, HCOOH, CH_4 and C_2H_4 were increased at the relatively negative potentials. At that moment, CH_4 and C_2H_4 became the dominant products at a sufficiently negative potential (< -1.0 V vs. RHE).

Based on the previous experiments, Nørskov et al. utilized the computational hydrogen electrode (CHE) model and den sity functional theory (DFT) calculations to explain the catalytic reactions on Cu catalysts[17]. The free energy diagrams exhibited the lowest-energy pathways for H_2 and C1 (CO, CH_4 and COOH) products on Cu (211) surface (Fig. 1). It shows that CO is a key intermediate to form CHO* with the addition of a proton-electron pair. If catalyst materials adsorb CHO* intermediate stronger than CO, the overpotential will be overwhelmingly reduced. The C-C coupling to form C2 products on Cu(211) surface was also explored in CO_2 electroreduction[18]. The $\Delta E_{a,elec}$, ΔH_a and ΔG_{rxn} represent the changes of electronic energy, enthalpy and Gibbs free energy, respectively (Tab. 2). At ambient temperature, $\Delta E_{a,elec}$ of two adsorbed *CO dimerization is higher than others and their ΔG_{rxn} is significantly positive. $\Delta E_{a,elec}$ and

ΔG_{rxn} hydrogenated derivatives of *CO (*CHO and *CH$_2$O) dimerization are relatively small, so that the steps need a lower overpotential. From the above results, the kinetic barriers indicate that the formation of C-C bond is feasible, and *CO direct dimerization is kinetically unsupported. This result is inconsistent with the previously *CO dimerization pathway[19]. Thus, *CO is protonated to form intermediates *CHO and *CH$_2$O firstly, and then C2 and C3 products could be produced at lower overpotentials.

Following this work, Jaramillo investigated 16 kinds of products for CO$_2$ electroreduction, the initially reported products were acetone, ethylene glycol, hydroxyacetone, glyoxal and glycolaldehyde, while 11 other kinds of products included C2 and C3 hydrocarbon or oxygenates, e.g., ethylene, *n*-propanol, allyl alcohol and ethanol (Fig. 2)[13]. CO and HCOOH were initially observed at the most positive potential of -0.65 V vs RHE, and CH$_4$ and C$_2$H$_4$ hydrocarbons were detected at -0.75 V vs. RHE. Subsequently, a
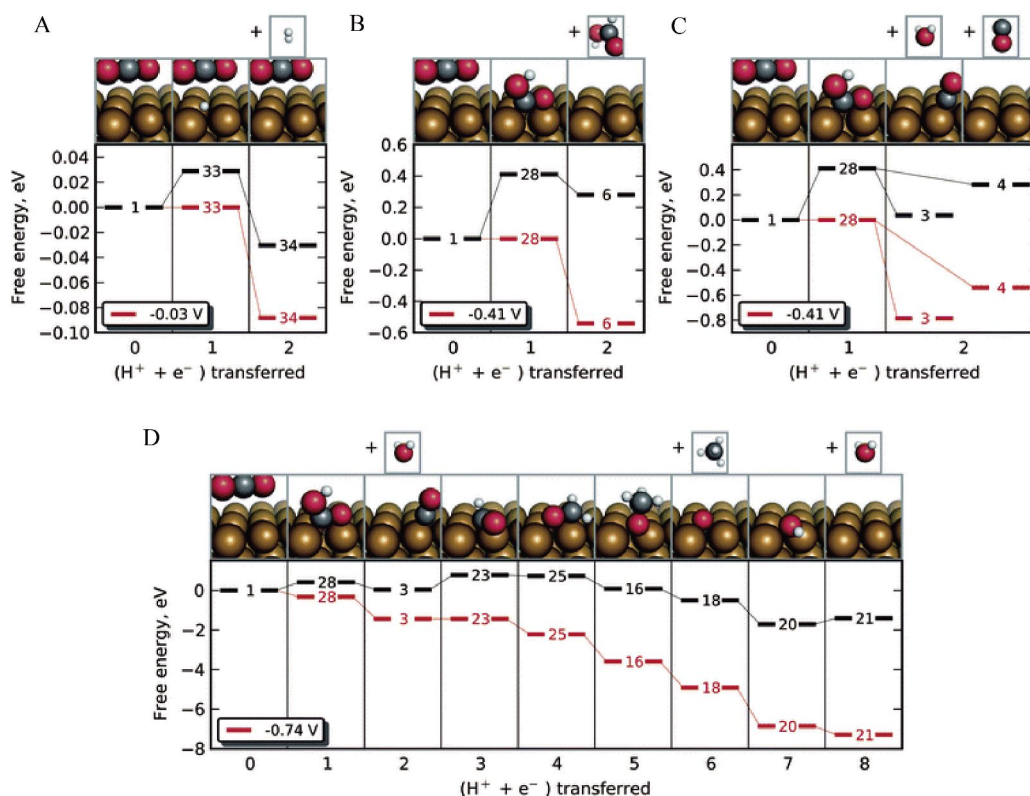
Fig. 1 The Free energy diagrams for the lowest energy pathways to (A) H$_2$, (B) HCOOH, (C) CO, and (D) CH$_4$. In each diagram, the black (higher) pathway represents the free energy at 0 V vs. RHE and the red (lower) pathway the free energy at the indicated potential. Reproduced with permission[17]. Copyright 2010, Royal Society of Chemistry.

Tab. 2 Electronic ($\Delta E_{a,elec}$), enthalpic barriers (ΔH_a) and reaction free energies (ΔG_{rxn}) on Cu(211). Reproduced with permission[18]. Copyright 2013, wiley-VCH.

Reaction	$\Delta E_{a,elec}$/eV	ΔH_a/eV	ΔG_{rxn}/eV
2*CO → O*C*CO	1.619	1.547	1.296
*CO + *CHO → O*C*CHO	0.675	0.683	0.177
2*CHO → *OCHCHO*	0.564	0.546	-1.198
*CHO + *CH$_2$O → *OCH$_2$CHO	0.374	0.422	-0.859
2*CH$_2$O → *OCH$_2$CH$_2$O	0.203	0.188	-1.028
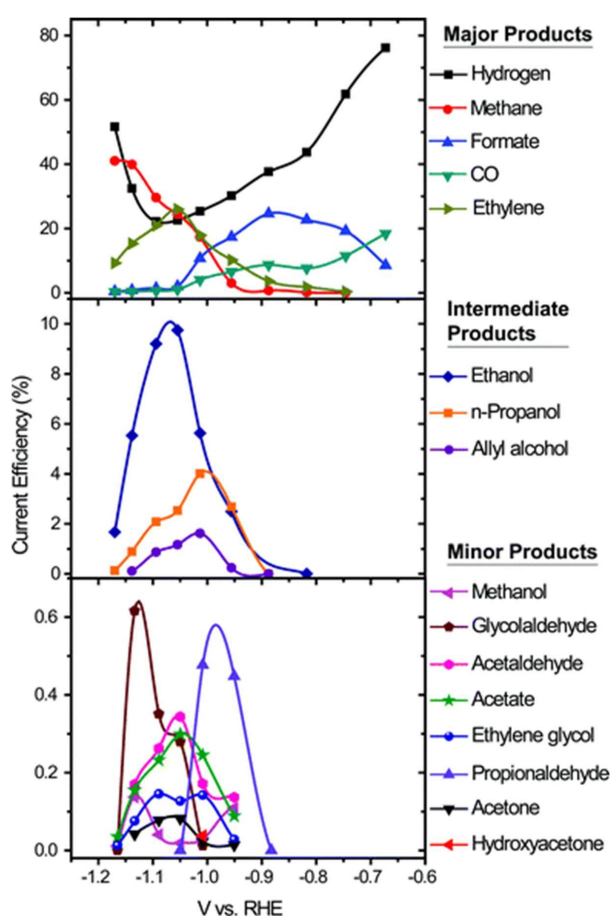
图 2　在不同电位下主要产物、中间产物和微量产物的电流效率[13]

Fig. 2　Current efficiency for each product as a function of potential for major, intermediate range, and minor products. Reproduced with permission[13]. Copyright 1989, The American Chemical Society.

large number of multicarbon products began to appear, while the *FE*s were first increased and then decreased with the increasing potential. C_2H_4 demonstrated the same trend, which indicated that one of the pathways to C_2H_4 was same as the pathways to C2 and C3 species. At the significantly negative potentials, H_2 and CH_4 dominated the CO_2 electroreduction products and the total current efficiencies exceeded 90%. Therefore, at the less negative potentials, proton and electron were favorably transferred. When the potential was very negative, C1 intermediates (e.g. *CO, *HCO, etc.) unfavorably form C-C bond and preferred to obtain CH_4 instead of C2, C3 species[20-23].

In the past decades, a lot of investigations were

done for CO_2 reduction on Cu-based catalysts, and many pathways and possible mechanisms are proposed. The *CO is suggested as the important intermediate on the pathways of CO_2 to hydrocarbons, while *CO is protonated and dimerized or *CO directly dimerized to form C2 products. However, there are many questions and confusion, more experiments and theoretical calculations are needed to clarify the mechanism to direct design the catalysts for practical use.

2　CO₂ Electrochemical Reduction on Cu-Based Catalysts

The major challenge of CO_2RR is to increase the selectivity for the target compounds along with the reduced overpotentials. The catalytic activity and product selectivity of CO_2RR are also determined by the morphology and structure of Cu catalysts. In this part, we will elaborate the relationship of morphology/structure, properties and their activities of various Cu catalysts from the structure, composition, modification and other emerging nanomaterials.

2.1　Dimensional Cu Materials

The physical morphology and structure significantly determine the surface and chemistry of catalyst. Then nanostructured Cu-based materials from zero-dimensional (0D) nanoparticles, one-dimensional (1D) nanowires/fibers/tubes, two-dimensional (2D) foils/layers/films/sheets, event three-dimensional (3D) foams/flowers and other superstructures have been investigated in CO_2RR. The first consideration is the size effect on the 0D Cu nanoparticles for the CO_2 conversion[24]. Results show that Cu nanoparticles in the range of 2 ~ 15 nm have an optimized influence on the catalytic activity of CO_2 conversion, while H_2 is the main product when the size is smaller than 30 nm (Fig. 3), which means that the hydrogen evolution dominates the water coupled CO_2 electrolysis. The *FE*s of both H_2 and CO increased with the decreased size of Cu nanoparticles, and the increasing tendency was dramatic for these smaller particles (< 5 nm). Meanwhile, the catalytic activity and selectivity of hydrocarbons (CH_4 and C_2H_4) were suppressed according-
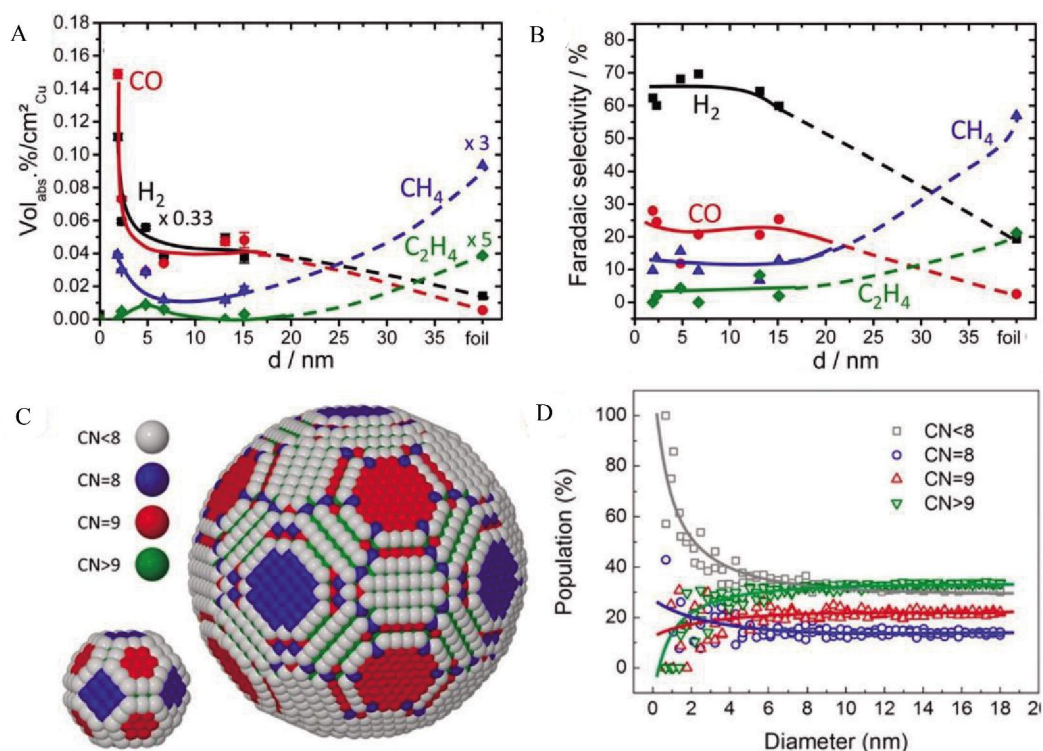
Fig. 3 Particle size dependence of (A) the composition of gaseous reaction products (balance is CO_2) during catalytic CO_2RR over Cu NPs, (B) the faradaic selectivity of reaction products during the CO_2RR on Cu NPs. (C) Ball models of spherical Cu NPs with 2.2 and 6.9 nm diameters. Surface atoms are color-coded according to their first neighbor coordination number (CN), CN < 8 (gray), CN = 8 (blue), CN = 9 (red), CN > 9 (green). (D) Population (relative ratio) of surface atoms with a specific CN as a function of particle diameter. Reproduced with permission[24]. Copyright 2014, The American Chemical Society.

ly. When the particles were less than 2 nm, the size effects were dramatically increased. A plausible explanation was proposed that small nanoparticles with plentiful low-coordinated atoms strongly bonded with the intermediates (CO and H), suppressing the further reaction to form hydrocarbons. On the contrary, *FE* of CH_4 could obtain 80% over 7 nm Cu nanoparticles and the partial current density of CH_4 was 4 times larger than that of pure Cu foil electrode[25]. With the increased Cu nanoparticles size (e.g., 50 ~ 100 nm), a high *FE* of 36% for C_2H_4 and an only 1% *FE* toward CH_4 were achieved on this Cu nanoparticle, because of weak binding of CO and H enhancing hydrocarbons formation[26].

Except the particle size, the morphologies of Cu catalysts also determine the surface Cu atoms arrangement and distribution. Hori and co-workers demonstrated that the CO_2 reduction products were dependent on the facets of Cu crystal, Cu(100) favored C_2H_4 production, while Cu(111) preferred to form CH_4 at the same potential[28-29]. In the early studies, Asthagiri employed the DFT calculations to evaluate the specific pathways of CO_2 reduction on the Cu(111) and Cu(100) facets[30-31]. According to the results, the conversion of *CO into *CHO or *COH was suggested as the key selective step. CH_4 and C_2H_4 were produced through *COH intermediate under the high overpotentials on the Cu(111) facets, which was consistent with the experimental results[32-33]. On the contrary, the formation of intermediate *CHO was favored on the Cu(100) facets. Then C_2H_4 and C_2H_5OH were produced due to the C-C bond formation of two *CHO under less negative potential. Those pathways were consistent with the reported experimental results, one pathway of C_2H_4 was similar to other C_2 oxygenates[13].

For example, cubic Cu nanoparticles revealed a high selectivity and low overpotential for C_2H_4, while the CH_4 was totally suppressed[34]. Loiudice et al. employed colloidal chemistry method and prepared different Cu nanocubes (24 nm, 44 nm and 63 nm) and Cu nanocrystal spheres (7.5 nm and 27 nm) for CO_2RR[27]. Generally, the Cu nanocubes were found more active than the Cu spheres. Cu nanocubes (44 nm) showed the highest efficiency for CO_2 reduction and the highest FE of 41% toward C_2H_4 production (Fig. 4). The Cu nanocube surface was made by Cu(100) facet and (100) steps, thus confirming that Cu(100) was favoring the formation of multicarbon products. Increasing the Cu cube size, the number of atoms on the plane increased, while the corner and edge atoms decreased relatively. Experimental results indicated that the balance between the edge sites and plane sites is vital for CO_2 reduction and C_2H_4 selectivity. Fig. 4 shows the specific CO_2 electroreduction pathways on the Cu (100) facet[19]. On the Cu(100) surface, the reaction pathway for the dimerization of two adsorbed *CO was demonstrated exprimentally to form C_2H_4[32-33, 35]. However, comparing the protonation of *CO to *CHO, the direct dimerization of *CO was unfavorable[19]. For these low-index terrace facets of Cu(100), Cu(111) and Cu(110), many researches illustrated the preferences of C_2H_4 for Cu(100) and CH_4 for Cu(111)[26, 36-38]. The high-index stepped surfaces

(Cu(711), Cu(511) and Cu(311)) all showed a higher selectivity of C_2H_4 and other C2, C3 productions. These stepped Cu facets needed lower overpotentials than the terrace surfaces and had different selectivities, as Cu step edges and kinks bind CO more strongly than the terrace surfaces[36-37, 39]. For example, Cu(711) surface contained mostly (100) terrace and some (111) step sites, and held an FE of 51.6% for C_2H_4 and 3.8% toward CH_4[19]. Obviously, theses corners, edges, steps and kinks were reaction active sites and made contributions to a high reaction activity (high current density)[24].

To enhance catalytic activity of CO_2 electroreduction, nanostructure engineering is often employed to enhance the structure-determined CO_2 performance on various Cu catalysts[38]. For example, dendritic Cu selectively formed C_2H_4 instead of CH_4, while honeycomb-like Cu with and 3D Cu foam produced a mixture of C_2 hydrocarbons (C_2H_4 and C_2H_6) and suppressed CH_4 formation at -1.9 V vs. Ag/AgCl[38]. However, some similar nanostructures of porous dendritic Cu were reported for converting CO_2 to HCOOH with a high selectivity of 90% and large current densities in water/ionic liquid mixture electrolyte[40]. Sen et al. reported a 3D hierarchical Cu nanofoam by electrodeposition on mechanically polished Cu substrates for the HCOOH production[41].

In addition, Chung et al. synthesized a series of
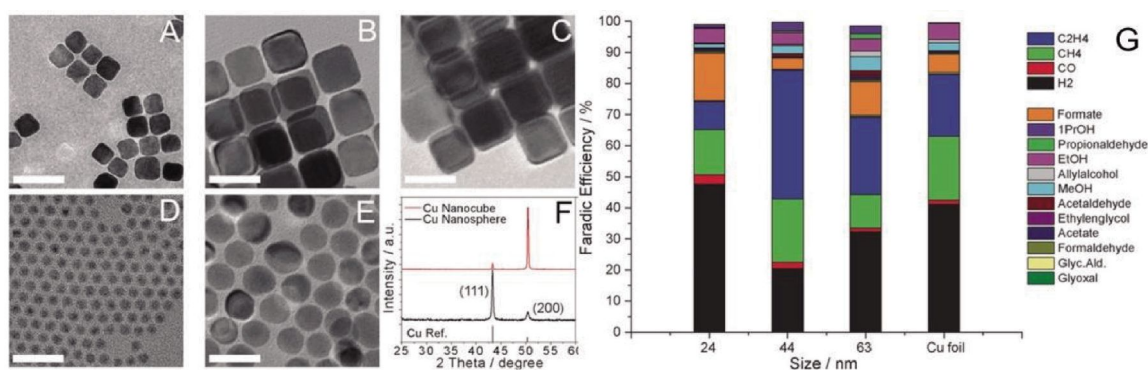
Fig. 4 (A-C) TEM images of Cu cubes with an average edge length of 24, 44, 63 nm, respectively; (D-E) TEM images of Cu spheres with an average diameter of 7.5 and 27 nm, respectively. Scale bar 50 nm. (F) Typical XRD patterns of the Cu spheres (black line) and Cu cubes (red line). (G) Bar graph reporting the faradaic efficiencies for each product in the different sizes of Cu NC cubes and in the Cu foil at -1.1 V vs. RHE. Reproduced with permission[27]. Copyright 2015, Wiley-VCH.

hierarchical Cu pillar electrodes by electrodeposition. The hierarchical Cu pillar electrode exhibited a selectivity to HCOOH with an *FE* of 28% at a potential of -0.5 V vs. RHE[42]. Kas et al. reported a 3D porous hollow fiber Cu electrode, which obtained a high *FE* of CO to ~ 72% at -0.4 V vs. RHE[43]. To increase the mass transfer and diffusion, porous hollow fiber Cu electrode was investigated in CO_2RR (Fig. 5A, B). The *FE* of CO of this porous fiber electrode was declined at more negative potential of -0.5 V and that may be ascribed to the desorption or further reaction of CO into other products at this potential (Fig. 5C). In the Tafel plot of CO, the first step was attributed to electron transfer to the adsorbed $*CO_2$ and the second Tafel slop was 93 mV·dec^{-1} closing to 116 mV·dec^{-1}, which suggested that the rate-determining step to form CO was the formation of *COOH inter- mediate (Fig. 5D).

2.2 Bimetallic Cu Catalysts

In order to improve the catalytic activity and selectivity for the conversion of CO_2, alloying is a favorable method to tune the binding strength of reaction intermediates on the Cu-based catalysts. Tin (Sn) is known to be a good metal catalyst for CO_2RR to HCOOH, but when it is doped into Cu, the products are changed. Yang et al. reported the Sn coating on Cu foam by electrodeposition method with the *FE* of 83.5% for CO at -1.8 V vs. Ag/AgCl[44]. Moreover, Sarfraz et al. investigated different amounts of Sn on the Cu surface. This kind of electrodes can convert CO_2 to CO with high catalytic activity and a maximum selectivity higher than 90% (-0.4 to -0.8 V vs. RHE) for a long period of time (> 14 h)[45]. The CO selectivity is dependent on the amounts of deposited
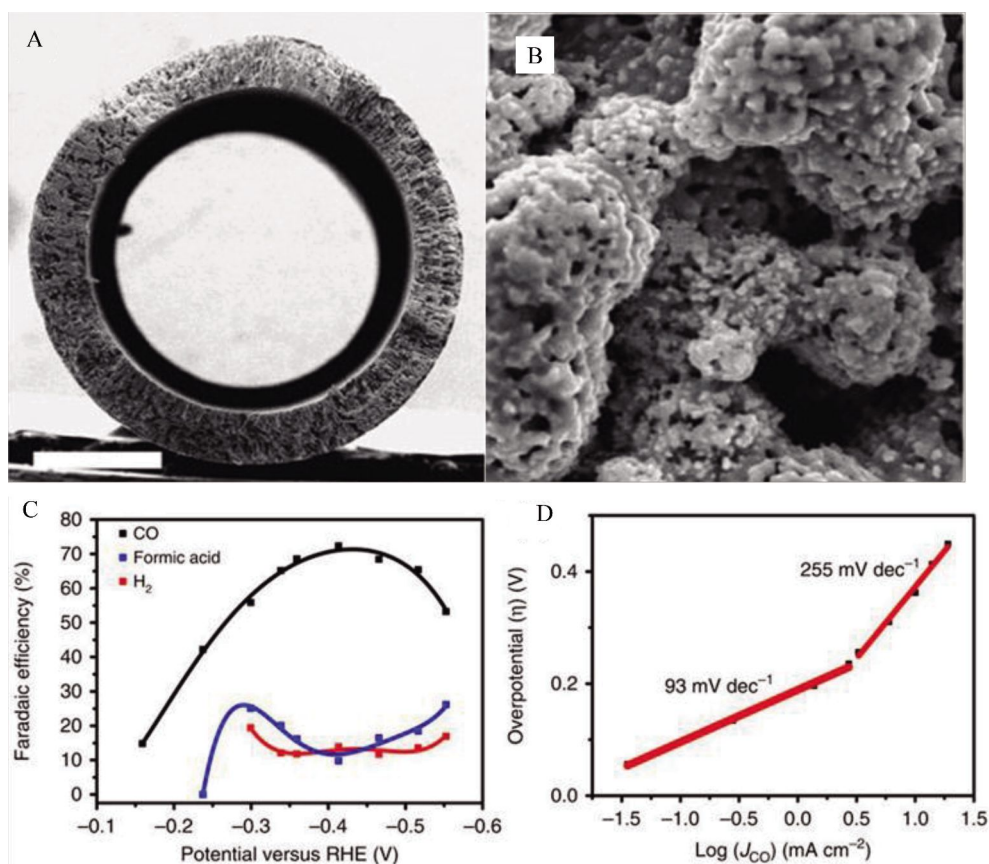
Fig. 5　(A) Cross-sectional image of a perpendicularly broken Cu hollow fiber. Scale bar, 100 μm. (B) High magnification of the outer surface of the Cu hollow fiber. (C) FE as a function of applied potential for CO, formic acid and H$_2$, using a CO$_2$ purge of 20 mL·min^{-1}. (D) Overpotential versus partial current density of CO using Cu hollow fiber. Reproduced with permission[43]. Copyright 2016, Nature Publishing Group.

Sn. Excess Sn diminishes the CO *FE*, while favors H_2 generation. Moreover, a thin layer of SnO_2 is coated over Cu nanoparticles, the thicker (1.8 nm) shell generates HCOOH, whereas the thinner (0.8 nm) shell favors CO with a 93% *FE* at -0.7 V (vs. RHE)[46]. So the optimal composition of Cu-Sn bimetal efficiently and selectively generates CO, but the surface of Cu-Sn bimetal with excess Sn shows Sn-like activity to generate HCOOH. For instance, Sn-based film with a thickness of ~ 325 nm on Cu foil showed a higher selectivity for HCOOH (91.5% at -1.8 V vs. Ag/AgCl) [47], Likewise, Yang et al. reported the Sn coating on Cu foam by electrodeposition for 35 min with an *FE* of 83.5% for HCOOH at -1.8 V vs. Ag/AgCl[44].

Like Sn, metal indium (In) also favors the production of HCOOH for CO_2RR, and Cu-In catalyst usually generates CO with the appropriate proportion due to the suppressed H_2 evolution by In atoms[48]. Rasul et al. reported that Cu-In alloys by electrochemical deposition selectively converted CO_2 toward CO with a high *FE* of 90% at -0.6 V vs. RHE along with extremely high stability in 0.1 mol·L^{-1} $KHCO_3$ [49]. From the DFT calculation results, In atoms prefer to be located on the edge sites instead of the corner or flat sites, and greatly influence the adsorption ability of neighboring Cu[50]. Moreover, other noble metals are also introduced to form Cu alloys, for instance, Cu-Au and Cu-Pd. Ma et al. investigated Cu-Pd alloy catalysts including ordered, disordered, phase-separated alloys (Cu_{at}:Pd_{at} = 1:1) and disordered Cu_3Pd and $CuPd_3$[51]. Ordered CuPd alloy had the highest selectivity toward CO product (*FE* > 60%) compared with other kinds of CuPd alloys (disordered and phase-separated alloys), while the phase-separated CuPd alloys possessed the highest selectivity to C_2 species (C_2H_4 and C_2H_5OH). With the increasing Cu/Pd ratio (Pd, $CuPd_3$, CuPd to Cu_3Pd and Cu), the *FE* of C2 products increased and the highest *FE* of C_2H_4 was obtained over 45% at only -0.8 V (Fig. 6). In addition, $PdCl_x$ decorated Cu nanoparticles achieved the *FE* of 30.1% for C_2H_6. Like alloyed Cu-Pd, Cu-Au catalysts with different compositions were also investigated[52-53].

With the increase of Cu content, more hydrocarbon products and the decreased CO were observed on the series of Cu-Au nanoparticle monolayers[53]. Besides, Jia et al. reported that the bimetal $Cu_{63.9}Au_{36.1}$ could catalyze CO_2 to polyols with the *FE* of 15.9% for CH_3OH and *FE* of 12% for C_2H_5OH[54]. Therefore, the geometric/structural and electronic effects could be realized by alloying Cu to tune the binding strength of intermediates on a catalyst surface, and thus enhance the activity and selectivity for CO_2RR.

2.3　Supported Cu Catalysts

Benefit from the tradition catalyst system, Cu catalysts are also fabricated by supporting Cu on the various substrates to disperse the active nanoparticles and expose sufficiently the active sites as the same time to increase the performance via the synergistic effect. For instance, a variety of carbon materials including pure graphite (PG), graphene oxide (GO), N-doped graphene, carbon nanotubes (CNTs) and carbon gel were employed to deposit Cu for CO_2RR. As increasing the Cu concentration, the electrochemical activity was increased and CH_4 was formed with a high *FE* of ~ 40% at high initial concentrations of Cu for both Cu/GO and Cu/PG catalysts[55]. Besides, the theoretical studies indicated that graphene-supported Cu could improve the catalytic ability, as the defect sites could anchor the Cu nanoparticle, thereby, increasing the stability and interaction of Cu-graphene system. Besides, the defect sites could also stabilize the reaction intermediates during CO_2RR process and prevent the agglomeration of Cu nanoparticles [56]. Thus, in order to improve the amount of defect sites and the catalytic activity, some studies applied the N-doped graphene as the supporting materials to locate Cu nanoparticles.

Song et al. synthesized Cu nanoparticle/N-doped graphene electrode[57], which efficiently converted CO_2 to C_2H_5OH with a high selectivity of 84% and a high *FE* of 63% at -1.2 V vs. RHE. Both the active Cu species and the synergistic interaction between Cu and neighboring carbon atoms contributed to the efficient electrochemical conversion of CO_2 to C_2H_5OH via carbon monoxide dimer pathway. Furthermore,
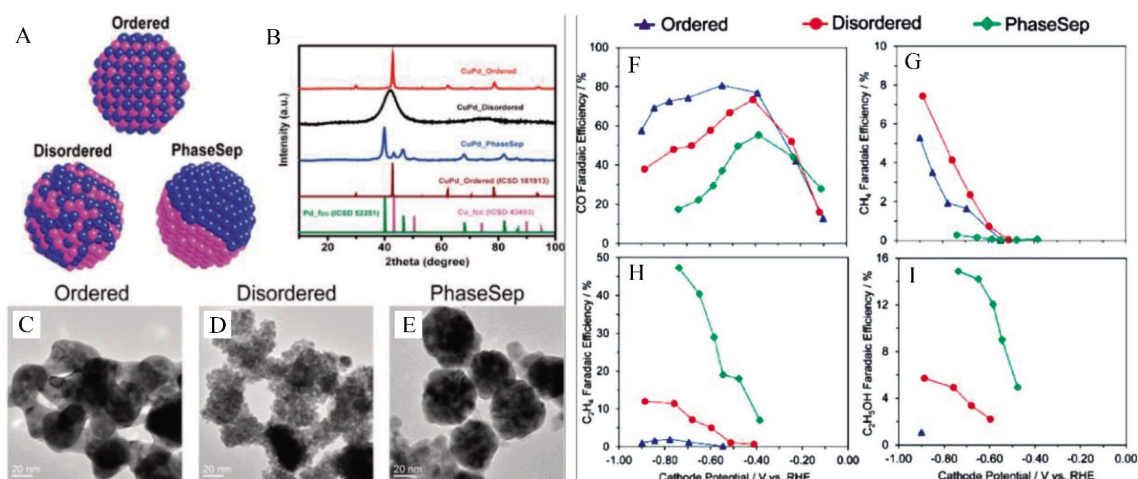
Fig. 6　(A) Illustration of prepared CuPd nanoalloys with different structures; (B) XRD patterns of prepared CuPd nanoalloys as well as previously reported Cu, Pd and CuPd alloys; (C, D, E) High-resolution TEM images. (F-I) Faradaic efficiencies for (F) CO; (G) CH_4; (H) C_2H_4; (I) C_2H_5OH for bimetallic Cu-Pd catalysts with different mixing patterns: ordered, disordered, and phase-separated. Reproduced with permission[51]. Copyright 2017, The American Chemical Society.

the carbon lattice inserted N, S or B, and the neighbor carbon atoms became the active sites. Li et al. reported Cu nanoparticles assembled on a pyridinic-N rich graphene (p-NG) support with an *FE* of 62% for HCOOH at -0.8 V and *FE* of 19% for C_2H_4 at -0.9 V vs. RHE. CO_2 and proton could be absorbed by the pyridinic-N functions, which promoted hydrogenation reaction to form C_2H_4 products[58]. Recently, Malik et al. investigated multi-wall carbon nanotubes (MWCNTs) with different Cu_2O loadings (10wt% ~ 50wt%). The catalyst with 30wt% Cu_2O could achieve a high current density and *FE* of 38% for CH_3OH at -0.8 V vs. RHE[59]. Similarly, CNT-supported Cu converted CO_2 to CH_3OH with an *FE* of 38.5%[60].

2.4 Derived Cu Catalysts

Except for the pure Cu catalysts, numerous functioned Cu-based catalysts such as oxide-derived Cu, copper(I) halide, copper(I) sulfide, alloy, carbon supported Cu and surface modified Cu have been reported for CO_2RR. These functioned Cu-based catalysts can enhance the catalytic activity and alter the selectivity of reduction products via electronic effect, strain effect and grain-boundary effect. *In-situ* electrochemical reductions of the CuO and Cu_2O materials, known as oxide-derived Cu catalysts, have been proven to greatly enhance the catalytic activity during

CO_2RR. Kanan and coworkers synthesized thick Cu_2O films by annealing Cu at 500 °C for 12 h. These films were formed by dense rods arrays with the diameters of 100 ~ 1000 nm[20]. The high *FE* of ~ 45% for CO production at potentials of -0.3 to -0.5 V vs. RHE and 33% for HCOOH production at potentials of -0.45 to -0.65 V vs. RHE were obtained (Fig. 7). The Tafel slope of 116 mV·dec^{-1} was consistent with a rate determining initial electron transfer to CO_2 to form a surface adsorbed $*CO_2^{·-}$ intermediate[29]. Moreover, the oxide-derived Cu nanowires by electrochemical reduction of CuO nanowires showed more advanced electrochemical activity and selectivity than by annealing under H_2 atmosphere, achieving the *FE* of 61.8% for CO production at -0.4 V and ~ 30.7% of HCOOH production at -0.6 V[61].

The intentional oxidation and reduction of copper electrodes are frequently employed to create active sites for the enhanced performance in CO_2RR. These oxides-derived Cu catalysts can convert CO_2 to not only two electrons products, but also multiple electrons hydrocarbons (C_2H_4, C_2H_6 and C_2H_5OH) with high selectivity. The Cu_2O-derived Cu nanoparticles with different initial crystal orientations or film thicknesses were investigated in CO_2RR. Results showed that the thickness of Cu_2O film dictated the reaction
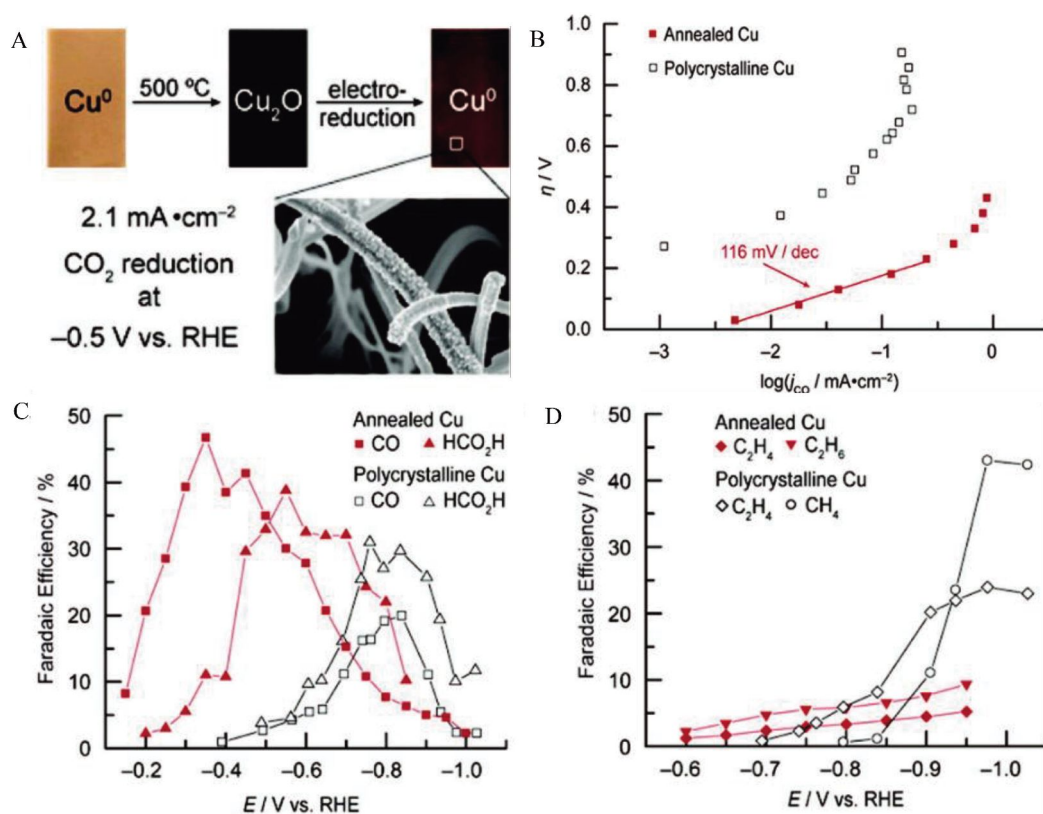
Fig. 7 (A) The color change of the catalyst during the reaction and the topography after the reaction. (B) Tafel plots for polycrystalline Cu and for Cu annealed at 500 °C for 12 h. (C) FE plots for CO and HCO_2H. (D) FE plots for CH_4, C_2H_4 and C_2H_6. Reproduced with permission[20]. Copyright 2012, The American Chemical Society.

selectivity, instead of the initial crystal orientation[62]. Under relative negative potential, the *FE* of hydrocarbon decreased, and the overall current density increased with the increasing Cu_2O film thickness, the highest *FE* of hydrocarbon exceeded 35% at -1.1 V vs. RHE. It was suggested that CO_2 reduction proceeded on newly *in-situ* formed Cu nanoparticles rather than Cu_2O film. Furthermore, additional research specified that the thickness of oxides-derived Cu was firmly related to the activity and selectivity of CO_2 reduction. Ren et al. investigated the copper (I) oxide films ranging from 0.2 to 8.8 μm, synthesized by electrochemical deposition[63]. The particle size increased along with the increasing thickness of Cu_2O film, the sizes of the particles were 0.2 μm and 8.8 μm when the thicknesses of the films were 100 nm and ~2 ~ 3 μm, respectively (Fig. 8). With the thickness ranging from 1.7 to 3.6 μm, the films suppressed the production of CH_4 (< 1% *FE*) and had a high se-

lectivity of C_2 hydrocarbons (34% ~ 39% *FE* of C_2H_4 and 9% ~ 16% *FE* of C_2H_5OH). The metallic Cu(0) was the catalytic active specie in CO_2 reduction process, which was consistent with the previous studies. In addition, the selectivity of C2 hydrocarbons exhibited a close relationship with pore size of the mesoporous Cu catalysts, and the high selectivity toward C2 production was maximal on the mesoporous oxides-derived Cu between 50 and 100 μm with the highest *FE* of 55% for C_2 hydrocarbons (C_2H_4 and C_2H_6)[64].

Except the reduced Cu species, some studies indicate that the grain boundaries in catalyst would be the active sites for CO_2 reduction[20, 65-66]. It is believed that the produced high local pH during the CO_2RR was favorable for the C_2H_4 production on the rough surface[15, 67-68]. Moreover, the presence of Cu^+ and residual subsurface oxygen have been suggested to influence the formation of C_2 productions, which is more
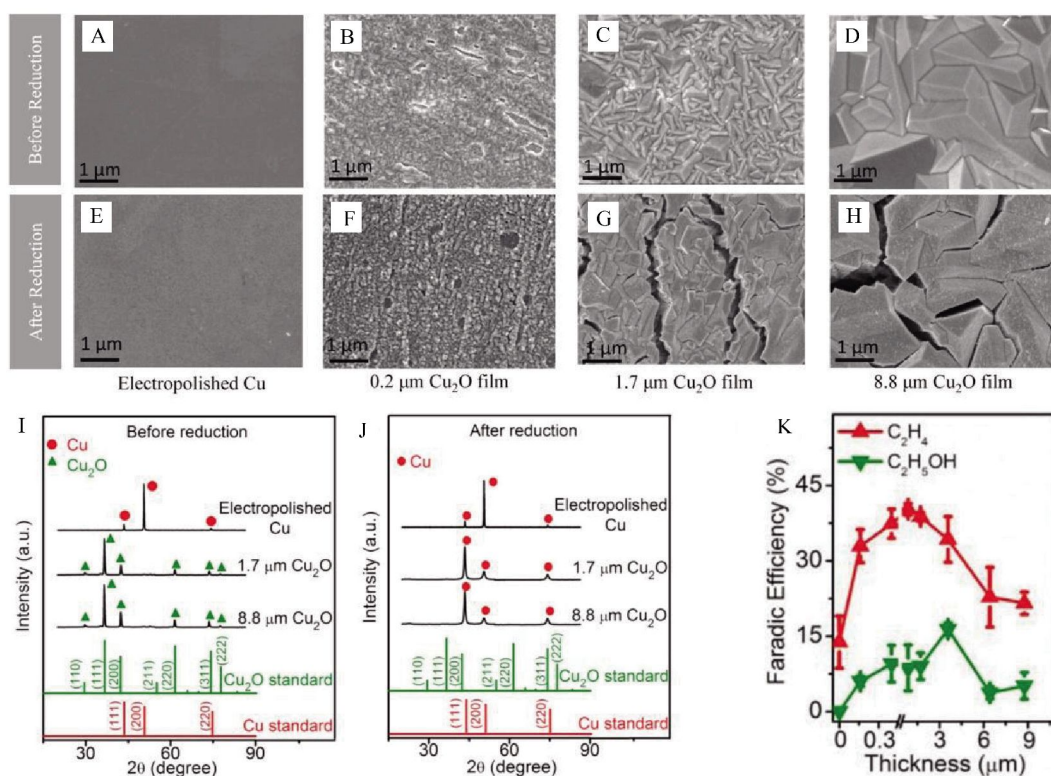
Fig. 8 SEM images of Cu catalysts before CO₂ reduction: (A) electropolished Cu; (B) 0.2 μm, (C) 1.7 μm, and (D) 8.8 μm Cu₂O films deposited on Cu disc. SEM images of Cu catalysts after CO₂ reduction at -0.99 V: (E) electropolished Cu; (F) 0.2 μm, (G) 1.7 μm, and (H) 8.8 μm Cu₂O films deposited on Cu disc. XRD patterns of Cu catalysts (I) before and (J) after CO₂ reduction. (K) *FE* plots for C₂H₄ and C₂H₅OH for 1.7-3.6 Cu₂O films deposited on Cu disc. The standard lines are also included in (I-J) for comparison (PDF 00-003-0892 for Cu₂O and PDF 00-001-1242 for Cu). Reproduced with permission[63]. Copyright 2015, The American Chemical Society.

important than the structural factors, such as roughness effects, defects, and grain boundaries[69-70]. Mistry et al. provided experiment results to support Cu⁺ as the active site for reducing CO₂ to C₂H₄[69]. These plasma-oxidized catalysts decreased the overpotential for CO₂ reduction products (CO, C₂H₄ and HCOOH) and the selectivity of C₂H₄ surprisingly reached 60% at only -0.9 V vs. RHE (Fig. 9). Cu⁺ always remained stable in Cu catalyst either before or after reduction during the electroreduction. These studies suggested that Cu⁺ was the key factor for decreasing the overpotential of CO₂ reduction and improving the selectivity of C₂H₄ rather than surface roughness and pH effects.

OD-Cu materials were special for CO₂RR and had great electrocatalytic performance to generate hydrocarbon, especially high carbon products. The catalysts were formed by reducing oxidized copper mate-

rials, and *in-situ* and *ex-situ* measurements indicated that the oxygen still existed. Nillson found that the subsurface oxygen induced high CO binding energy, and this could increase the CO coverage on catalyst surface, which kinetically enhanced the C-C bond formation to form the high carbon productions [71]. Thus, the roles of Cu⁺ species and oxygen in Cu catalyst attract enough attention, and the *in-situ* detection technologies should be largely used in CO₂RR to reveal evolution of the catalysts and the reaction intermediates, this is very important to design high efficiency catalyst and reveal the reaction mechanism.

2.5 Modified Cu Catalysts

Surface structure and electronic condition are important for the selective and active conversion of CO₂. Cu surface functionalization strategy could be effective to modify the surface electronic state and
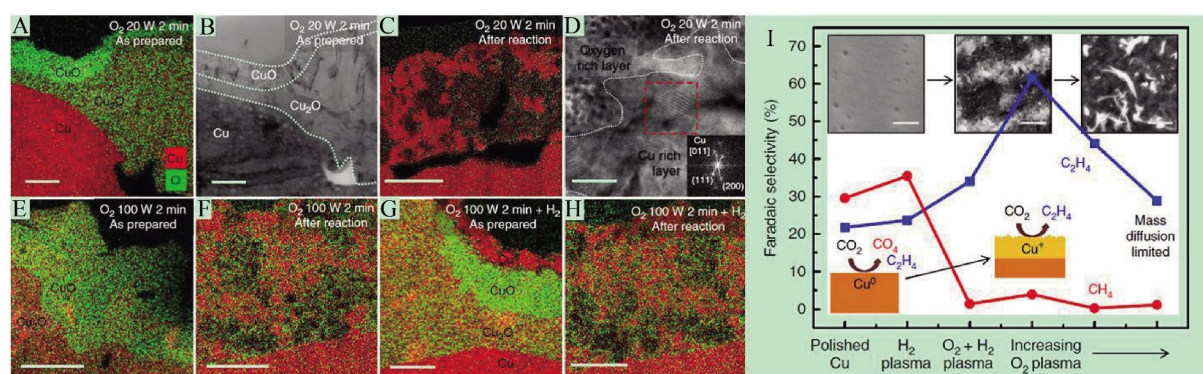
Fig. 9　EDS elemental maps of Cu foils treated with plasma under (A-D) 20 W for 2 min; (E-F) 100 W for 2 min; and (G-H) 100 W for 2 min + H_2 plasma. (I) FEs for the different materials. Reproduced with permission[69]. Copyright 2016, Nature Publishing Group.

chemistry, as these functional groups could tune the adsorption/desorption of the reaction intermediate, and thus, change the reaction pathway. For example, when the oleic acid (OA) ligand was functionalized on the Cu_2O and CuO nanoparticles, only CH_3OH and CO were produced, respectively[72]. Another example is amino acid modified Cu electrodes for CO_2RR[14]. The Cu nanowire film modified with glycine exhibited excellent activity for C2-C3 hydrocarbons (C_2H_6, C_2H_4 and C_3H_6) with 34.1% FE at -1.9 V vs. RHE (Fig. 10). The results indicated that CHO* and -NH_3^+ formed the hydrogen bond and CHO* were stabilized, which would contribute to high activity and selectivity of multi-carbon products.

2.6　Cu Complex Catalysts

The organic ligands are also used to combine Cu species and form molecular Cu complexes, and these ligands could stabilize Cu species and contribute the modification of intermediates. Moreover, the molecular catalyst is monophasic system, which endows the easy way to explore the catalytic mechanism[73-74]. Recently, Wang et al. reported a heterogeneous molecular Cu with porphyrin complex PorCu（copper（Ⅱ） 5,10,15,20-tetrakis (2,6-dihydroxyphenyl) porphyrin) for reducing CO_2 into hydrocarbons[75]. At -0.976 V vs. RHE, the total FE increased from 42% to 54% and the current density increased from 11 to 48 mA·cm^{-2} with time increasing (Fig. 11). Both high activity and selectivity for hydrocarbons (CH_4 and C_2H_4) demon-

strated by this molecular catalyst was attributed to the built-in hydroxyl groups in the Cu porphyrin complex.

Employ organic ligands could be constructed into metal-/covalent-organic frameworks (MOF/COF). These systems combine the advantages of monophasic molecular and heterogeneous catalysts with the abilities of tunable chemical structures, which possibly bring the high carbon number products[71]. For example, Cu rubeanate metal organic framework (CR-MOF) demonstrated the interesting HCOOH product at -1.2 V vs. SHE[76]. Apparently, the excellent electronic conductivity, proton conductivity, and dispersed reaction sites in the porous CR-MOF contributed to the good catalytic activity. Another kind MOF of $Cu_3(BTC)_2$ (BTC=1,3,5-benzenetricarboxylic acid) demonstrated the selective reduction of CO_2 to oxalic acid with the FE of 51%[77]. Furthermore, Lin et al. reported a variety of cobalt/copper porphyrins COF composites, COF-367-M （Co, Co/Cu (10/90), Co/Cu （1/99）). With the increasing Cu/Co ratio, the turnover frequency (TOF) was increased, while the FE of CO was decreased[78]. The turnover number (TON) of COF-367-Co（1%）was over 24000, and it is one of the most efficient catalysts reported to date for CO_2RR. Besides, Cu-MOF or Cu/M-MOF is outstanding sacrificial precursors to synthesize various functional nanostructures Cu-based materials by post-processing. Therefore, Cu-based MOF/COFs provide a new opportunity and platform for designing
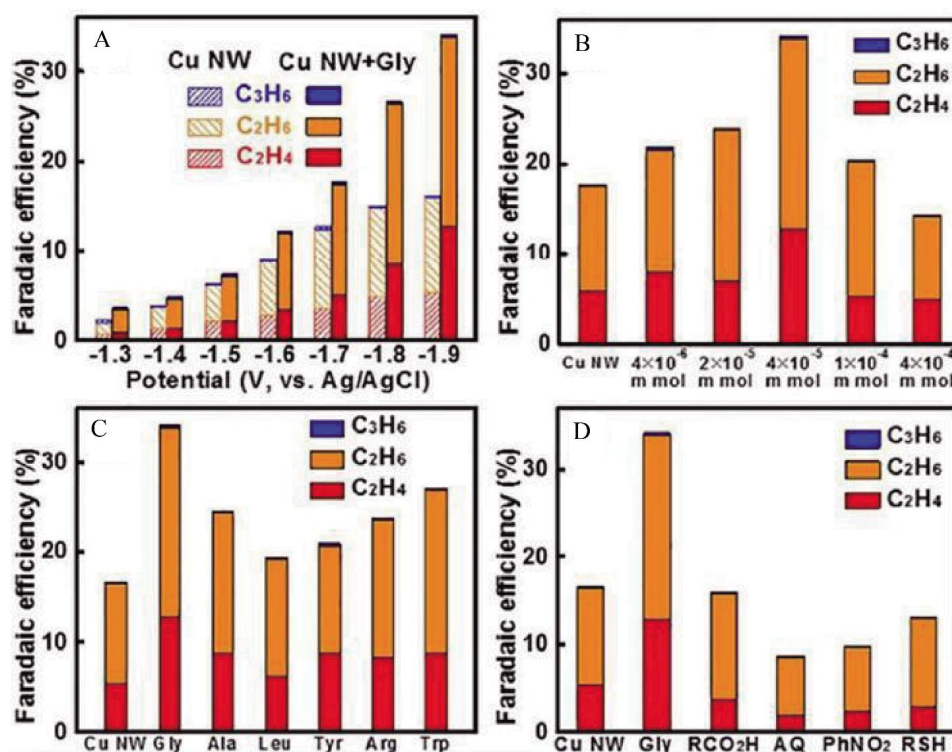
Fig. 10　Electrochemical CO₂ reduction on Cu NW film electrodes. (A) In the full potential range from -1.3 V to -1.9 V. (B) With different concentrations of glycine at -1.9 V. (C) With different kinds of amino acids at -1.9 V. (D) With different kinds of modifiers at -1.9 V. Reproduced with permission[14]. Copyright 2016, Royal Society of Chemistry.

efficient CO₂RR electrocatalysts.

3　Summary and Outlook

　　Various catalysts for CO₂RR have been intensively investigated to obtain both efficient catalytic activity and product selectivity for practical applications. Cu-based materials are the only metal material to produce a great deal of multi-carbon products with high activity and selectivity in CO₂RR. In this work, we summarized recent advances in copper-based materials for electrochemical CO₂ conversion. Moreover, the reaction mechanisms of CO₂ electroreduction on Cu-based catalysts are also discussed. Although the development of Cu-based CO₂RR electrocatalysts have been accelerated by massive experiments and theoretical calculations, yet many challenges to be overcome for efficient conversion of CO₂ to desirable products. Substantial Cu-based catalysts have shown significantly high overpotential, low catalytic activity and selectivity to produce multi-carbon products, as well as poor stability for only a few

hours. Moreover, the complete, accurate and clear CO₂ electroreduction mechanism and kinetics are not explicit yet for this complex process. Therefore, substantial scientific research should be performed to solve for these problems and achieve the goal of commercialization.

　　Firstly, multifarious Cu-based catalysts should be investigated to achieve high catalytic activity and stability, as well as the partial current density of target products should be enhanced. Nanostructured catalysts and composite materials are good development direction. Moreover, the reaction pathways of CO₂ electroreduction process are very complicated, and the understanding in the mechanisms of CO₂RR is inevitably required for the advancement of CO₂RR. In addition, some derived Cu catalysts, maybe named as "pre-catalyst", will suffer the evolution during the cathodic reduction process. Thus, a large amount of *in-situ* and advanced characterization technologies should be widely used to directly observe the reaction
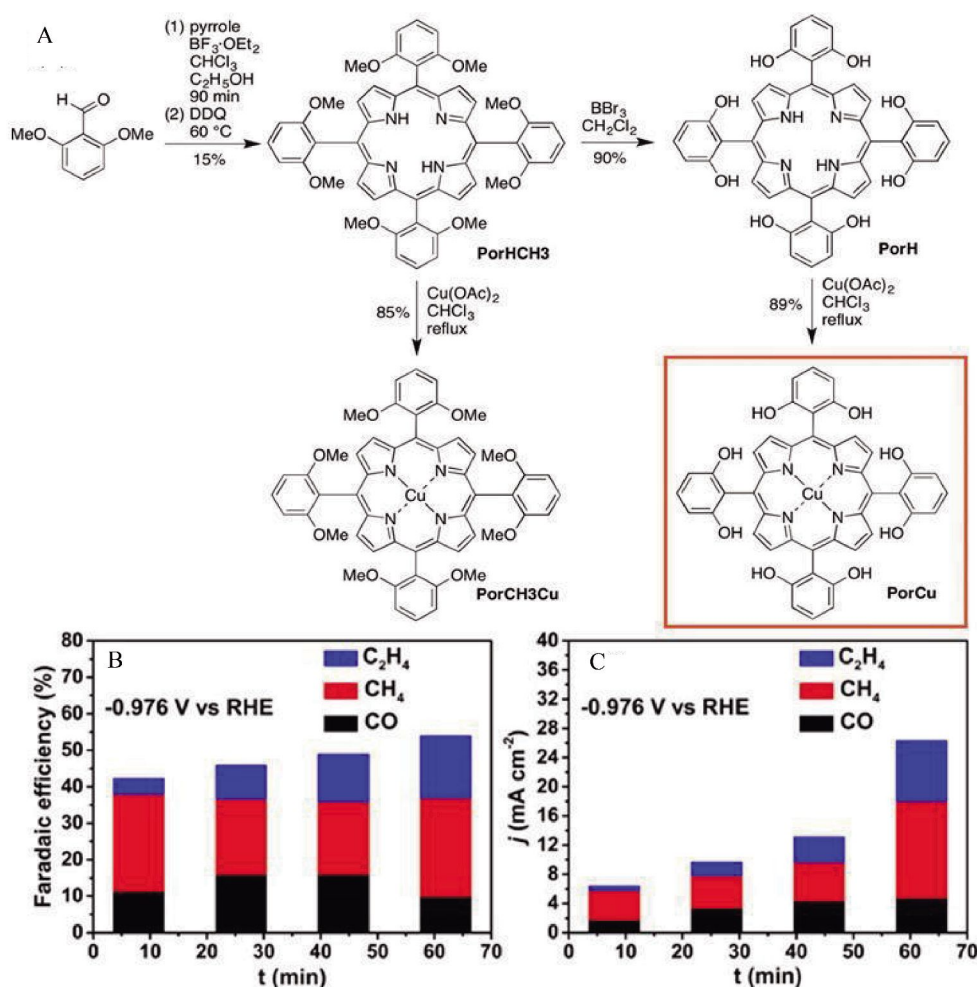
Fig. 11 (A) Synthetic routes for copper-porphyrin molecular catalysts. (B) Distribution of CO_2 reduction products in the gas phase as the electrolysis proceeded at -0.976 V vs. RHE. (C) The current density of CO_2 reduction products in the gas phase as the electrolysis proceeded at -0.976 V vs. RHE. Reproduced with permission[75]. Copyright 2016, The American Chemical Society.

intermediates and the change of catalyst to explore the reaction process, such as in operando spectroscopy and microscopy to monitor the intermediation of CO_2 reduction and the remolding of Cu catalyst in the real operation. Besides, computer technology and theoretical calculations are powerful tools to investigate the CO_2RR process at an atomic level. The combination of experiment, atomic structure, the interaction between reaction intermediates and catalyst surface could offer a deep insight to understanding the CO_2RR mechanism on Cu-based materials. In turn, those can provide valuable clues and help to design the Cu-based catalysts for highly efficient CO_2 conversion.

In the end, CO_2 electroreduction technology should achieve industrial application, which can reduce environmental issues and increase energy uses. The relatively low solubility of CO_2 in aqueous solutions leads to a mass transfer constraint. In order to achieve a higher catalytic efficiency and higher current density, the gas diffusion electrode (GDE) would be employed to effectively reduce the CO_2 mass transfer constraint. This goes directly to the gas phase instead of the liquid phase, and the flow cell replacing experimental Lab-level H-cell configuration is necessary. Therefore, a performance summarization of the Cu-based catalysts discussed in this review along with their reaction conditions is presented in

Tab. 3 The performance of recently reported Cu-based electrocatalysts for CO_2 reduction

Catalyst	Electrolyte	Potential/ V(vs. RHE)	Product (Faradaic efficiency)/%	Current Density/ (mA·cm^{-2})	Reference
Cu nanoparticles (10 nm)	0.1 mol·L^{-1} KHCO$_3$	-1.1	CO (22%), CH$_4$ (10%), C$_2$H$_4$ (4%)	20	[24]
Cu nanoparticles capped with tetradecylphosphonate of diameter 7.0 nm	0.1 mol·L^{-1} NaHCO$_3$	-1.25	CH$_4$ (80%)	9	[25]
Oxide derived Cu	0.5 mol·L^{-1} NaHCO$_3$	-0.5	CO (40%) HCOOH (33%)	2.7	[20]
Au$_3$Cu alloy	0.1 mol·L^{-1} KHCO$_3$	-0.73	CO (40%) HCOOH (3.11%)	3	[53]
CuIn alloy	0.1mol·L^{-1} KHCO$_3$	-0.6	CO (38%) HCOOH (34%)	1	[49]
Cu-MOF	0.5 mol·L^{-1} KHCO$_3$	-1.2 V/ (vs. SHE)	HCOOH (98%)	7.5	[76]
Cu$_{11}$In$_9$ on Cu foil	0.5 mol·L^{-1} KHCO$_3$	-0.6	CO (90%)	0.6	[49]
CuO derived Cu nanowire arrays	0.1 mol·L^{-1} KHCO$_3$	-0.41	CO (61.8%)	1	[79]
Cu$_2$O derived Cu nanorod arrays	0.5 mol·L^{-1} NaHCO$_3$	-0.5	CO (45%) HCOOH (33%)	2.7	[20]
15 nm thick Cu overlayers on Pt	0.1 mol·L^{-1} KHCO$_3$	-1.0	CH$_4$ (33%)	10	[80]
Cu nanparticles (50 ~ 100 nm)	0.1 mol·L^{-1} KClO$_3$	-1.1	C$_2$H$_4$ (36%)	Non	[26]
Carbon supported 12 nm Cu nanoparticles	0.1 mol·L^{-1} KHCO$_3$	-0.9	C$_2$H$_4$ (19%)	7.5	[14]
Ru/Cu alloy	0.5 mol·L^{-1} NaHCO$_3$	-0.8 V/ (vs. SCE)	CH$_3$OH (41.3%)	0.04	[81]
Cu electrode	Organic lithium salt sysytem	-1.1 (vs. Ag/AgCl)	CH$_3$OH (40%)	9	[82]
Cu nanoparticles on N-doped carbon nanospkikes	mol·L^{-1} KOH	-1.2	C$_2$H$_5$OH (63%)	2	[57]
Cu electrode	0.1 mol·L^{-1} KClO$_3$	-1.4 V (vs. NHE)	C$_2$H$_4$ (48.1%)	5	[83]
Cu electrode	0.08 mol·L^{-1} CsOH/methanol	-3.5 V (vs. Ag/AgCl)	C$_2$H$_4$ (32.3%)	11	[84]
Cu(100)	0.5 mol·L^{-1} NaHCO$_3$	-1.42 V (vs. NHE)	C$_2$H$_4$ (31.7%)	5	[85]
Cu nanocubes with 44 nm edge length	0.1 mol·L^{-1} KHCO$_3$	-1.1	C$_2$H$_4$ (41%)	5.6	[27]

Tab. 3 for comparison.

In summary, Cu-based materials are the most notable catalysts with high catalytic activity for hydrocarbons. This article has introduced the proposed CO$_2$RR mechanisms on Cu metal surface, and the re-

cent progress in Cu-based catalysts. Although many pathways and possible mechanisms have been proposed for CO$_2$RR over Cu-based catalysts in the past decades, there are still many questions and confusion, and more experimental results and theoretical calcu-

lations are stilled needed to clarify the concert mechanism and guide the design and preparation of efficient catalysts for practical application. More extensive efforts will be made, we believe, the development of CO_2RR could be swifter in the near future, and relatively cheap and practical catalysts for electrochemical CO_2 reduction would be obtained to achieve industrial application.

References:

[1] Goeppert A, Czaun M, Jones J P, et al. Recycling of carbon dioxide to methanol and derived products-closing the loop[J]. Chemical Society Reviews, 2014, 43(23): 7995-8048.

[2] Costentin C, Robert M, Savéant J M. Catalysis of the electrochemical reduction of carbon dioxide[J]. Chemical Society Reviews, 2013, 42(6): 2423-2436.

[3] Lu Q, Jiao F. Electrochemical CO_2 reduction: Electrocatalyst, reaction mechanism, and process engineering[J]. Nano Energy, 2016, 29: 439-456.

[4] Appel A M, Bercaw J E, Bocarsly A B, et al. Frontiers, opportunities, and challenges in biochemical and chemical catalysis of CO_2 fixation[J]. Chemical Reviews, 2013, 113 (8): 6621-6658.

[5] Li H(李宏), Cai W B(蔡文斌). Interaction between energy and electrocatalysis[J]. Journal of Electrochemistry(电化学), 2018, 24(2): 194-196.

[6] Kondratenko E V, Mul G, Baltrusaitis J, et al. Status and perspectives of CO_2 conversion into fuels and chemicals by catalytic, photocatalytic and electrocatalytic processes [J]. Energy & Environmental Science, 2013, 6(11): 3112-3135.

[7] Cao Z, Zacate S B, Sun X D, et al. Tuning gold nanoparticles with chelating ligands for highly efficient electrocatalytic CO_2 reduction[J]. Angewandte Chemie International Edition, 2018, 130(39): 12857-12861.

[8] Gabardo C M, Seifitokaldani A, Edwards J P, et al. Combined high alkalinity and pressurization enable efficient CO_2 electroreduction to CO[J]. Energy & Environmental Science, 2018, 11(9): 2531-2539.

[9] Geng Z G, Kong X D, Chen W W, et al. Oxygen vacancies in ZnO nanosheets enhance CO_2 electrochemical reduction to CO[J]. Angewandte Chemie International Edition, 2018, 57(21): 6054-6059.

[10] Lei F C, Liu W, Sun Y F, et al. Metallic tin quantum sheets confined in graphene toward high-efficiency carbon dioxide electroreduction[J]. Nature Communications, 2016, 7: 12697.

[11] Han N, Wang Y, Yang H, et al. Ultrathin bismuth nanosheets from *in situ* topotactic transformation for selective electrocatalytic CO_2 reduction to formate[J]. Nature Communications, 2018, 9(1): 1320.

[12] Gao D F, Zhou H, Cai F, et al. Pd-containing nanostructures for electrochemical CO_2 reduction reaction[J]. ACS Catalysis, 2018, 8(2): 1510-1519.

[13] Kuhl K P, Cave E R, Abram D N, et al. New insights into the electrochemical reduction of carbon dioxide on metallic copper surfaces[J]. Energy & Environmental Science, 2012, 5(5): 7050-7059.

[14] Xie M S, Xia B Y, Li Y, et al. Amino acid modified copper electrodes for the enhanced selective electroreduction of carbon dioxide towards hydrocarbons[J]. Energy & Environmental Science, 2016, 9(5): 1687-1695.

[15] Varela A S, Kroschel M, Reier T, et al. Controlling the selectivity of CO_2 electroreduction on copper: The effect of the electrolyte concentration and the importance of the local pH[J]. Catalysis Today, 2016, 260: 8-13.

[16] Hori Y, Murata A, Takahashi R. Formation of hydrocarbons in the electrochemical reduction of carbon dioxide at a copper electrode in aqueous solution[J]. Journal of the Chemical Society, Faraday Transactions 1, 1989, 85(8): 2309-2326.

[17] Peterson A A, Abild-Pedersen F, Studt F, et al. How copper catalyzes the electroreduction of carbon dioxide into hydrocarbon fuels[J]. Energy & Environmental Science, 2010, 3(9): 1311-1315.

[18] Montoya J H, Peterson A A, Nørskov J K. Insights into C-C coupling in CO_2 electroreduction on copper electrodes[J]. ChemCatChem, 2013, 5(3): 737-742.

[19] Luo W J, Nie X W, Janik M J, et al. Facet dependence of CO_2 reduction paths on Cu electrodes[J]. ACS Catalysis, 2016, 6(1): 219-229.

[20] Li C W, Kanan M W. CO_2 reduction at low overpotential on Cu electrodes resulting from the reduction of thick Cu_2O films[J]. Journal of the American Chemical Society, 2012, 134(17): 7231-7234.

[21] Qiao J l, Jiang P, Liu J S, et al. Formation of Cu nanos-

tructured electrode surfaces by an annealing-electrore-duction procedure to achieve high-efficiency CO_2 elec-troreduction[J]. Electrochemistry Communications, 2014, 38: 8-11.

[22] Tang W, Peterson A A, Varela A S, et al. The importance of surface morphology in controlling the selectivity of poly-crystalline copper for CO_2 electroreduction[J]. Physical Chemistry Chemical Physics, 2012, 14(1): 76-81.

[23] Chen C S, Handoko A D, Wan J H, et al. Stable and selec-tive electrochemical reduction of carbon dioxide to ethy-lene on copper mesocrystals[J]. Catalysis Science & Tech-nology, 2015, 5(1): 161-168.

[24] Reske R, Mistry H, Behafarid F, et al. Particle size effects in the catalytic electroreduction of CO_2 on Cu nanoparti-cles[J]. Journal of the American Chemical Society, 2014, 136(19): 6978-6986.

[25] Manthiram K, Beberwyck B J, Alivisatos A P. Enhanced electrochemical methanation of carbon dioxide with a dis-persible nanoscale copper catalyst[J]. Journal of the Amer-ican Chemical Society, 2014, 136(38): 13319-13325.

[26] Tang W, Peterson A A, Varela A S, et al. The importance of surface morphology in controlling the selectivity of polycrystalline copper for CO_2 electroreduction[J]. Physi-cal Chemistry Chemical Physics, 2012, 14(1): 76-81.

[27] Loiudice A, Lobaccaro P, Kamali E A, et al. Tailoring copper nanocrystals towards C2 products in electro-chemical CO_2 reduction[J]. Angewandte Chemie Interna-tional Edition, 2016, 55(19): 5789-5792.

[28] Yoshio H, Katsuhei K, Shin S. Production of CO and CH_4 in electrochemical reduction of CO_2 at metal electrods in aqueous hydrogencarbonate solution[J]. Chemistry Letters, 1985, 14(11): 1695-1698.

[29] Gattrell M, Gupta N, Co A. A review of the aqueous elec-trochemical reduction of CO_2 to hydrocarbons at copper [J]. Journal of Electroanalytical Chemistry, 2006, 594(1): 1-19.

[30] Baturina O A, Lu Q, Padilla M A, et al. CO_2 electroreduc-tion to hydrocarbons on carbon-supported Cu nanoparti-cles[J]. ACS Catalysis, 2014, 4(10): 3682-3695.

[31] Nie X W, Esopi M R, Janik M J, et al. Selectivity of CO_2 reduction on copper electrodes: The role of the kinetics of elementary steps[J]. Angewandte Chemie International Edition, 2013, 125(9): 2519-2522.

[32] Schouten K J P, Kwon Y, Van Der Ham C J M, et al. A new mechanism for the selectivity to C1 and C2 species in the electrochemical reduction of carbon dioxide on copper electrodes[J]. Chemical Science, 2011, 2(10): 1902-1909.

[33] Schouten K J P, Qin Z, Pérez Gallent E, et al. Two path-ways for the formation of ethylene in CO reduction on single-crystal copper electrodes[J]. Journal of the Ameri-can Chemical Society, 2012, 134(24): 9864-9867.

[34] Roberts F S, Kuhl K P, Nilsson A. High selectivity for ethylene from carbon dioxide reduction over copper nanocube electrocatalysts[J]. Angewandte Chemie Inter-national Edition, 2015, 54(17): 5179-5182.

[35] Kortlever R, Shen J, Schouten K J P, et al. Catalysts and reaction pathways for the electrochemical reduction of carbon dioxide[J]. The Journal of Physical Chemistry Let-ters, 2015, 6(20): 4073-4082.

[36] Hori Y, Takahashi I, Koga O, et al. Selective formation of C2 compounds from electrochemical reduction of CO_2 at a series of copper single crystal electrodes[J]. The Journal of Physical Chemistry B, 2002, 106(1): 15-17.

[37] Hori Y, Takahashi I, Koga O, et al. Electrochemical reduc-tion of carbon dioxide at various series of copper single crystal electrodes[J]. Journal of Molecular Catalysis A: Chemical, 2003, 199(1/2): 39-47.

[38] Gonçalves M R, Gomes A, Condeço J, et al. Electro-chemical conversion of CO_2 to C_2 hydrocarbons using different *ex situ* copper electrodeposits[J]. Electrochimica Acta, 2013, 102: 388-392.

[39] Takahashi I, Koga O, Hoshi N, et al. Electrochemical re-duction of CO_2 at copper single crystal Cu(S)-[n(111)× (111)] and Cu(S)-[n(110)×(100)] electrodes[J]. Journal of Electroanalytical Chemistry, 2002, 533(1): 135-143.

[40] Huan T N, Simon P, Rousse G, et al. Porous dendritic copper: an electrocatalyst for highly selective CO_2 reduc-tion to formate in water/ionic liquid electrolyte[J]. Chem-ical Science, 2017, 8(1): 742-747.

[41] Sen S, Liu D, Palmore G T R. Electrochemical reduction of CO_2 at copper nanofoams[J]. ACS Catalysis, 2014, 4(9): 3091-3095.

[42] Chung J, Won D H, Koh J, et al. Hierarchical Cu pillar electrodes for electrochemical CO_2 reduction to formic acid with low overpotential[J]. Physical Chemistry Chem-ical Physics, 2016, 18(8): 6252-6258.

[43] Kas R, Hummadi K K, Kortlever R, et al. Three-dimen-sional porous hollow fibre copper electrodes for efficient and high-rate electrochemical carbon dioxide reduction [J]. Nature Communications, 2016, 7: 10748.

[44] Wang Y, Zhou J, Lv W X, et al. Electrochemical reduc-tion of CO_2 to formate catalyzed by electroplated tin coat-ing on copper foam[J]. Applied Surface Science, 2016, 362: 394-398.

[45] Sarfraz S, Garcia-Esparza A T, Jedidi A, et al. Cu-Sn bi-

metallic catalyst for selective aqueous electroreduction of CO_2 to CO[J]. ACS Catalysis, 2016, 6(5): 2842-2851.

[46] Li Q, Fu J J, Zhu W L, et al. Tuning Sn-catalysis for electrochemical reduction of CO_2 to CO via the core/shell Cu/SnO_2 structure[J]. Journal of the American Chemical Society, 2017, 139(12): 4290-4293.

[47] Lv W X, Zhou J, Kong F Y, et al. Porous tin-based film deposited on copper foil for electrochemical reduction of carbon dioxide to formate[J]. International Journal of Hydrogen Energy, 2016, 41(3): 1585-1591.

[48] He J, Dettelbach K E, Salvatore D A, et al. High-throughput synthesis of mixed-metal electrocatalysts for CO_2 reduction[J]. Angewandte Chemie International Edition, 2017, 56(22): 6068-6072.

[49] Rasul S, Anjum D H, Jedidi A, et al. A highly selective copper-indium bimetallic electrocatalyst for the electrochemical reduction of aqueous CO_2 to CO[J]. Angewandte Chemie International Edition, 2015, 54(7): 2146-2150.

[50] Larrazábal G O, Martín A J, Mitchell S, et al. Enhanced reduction of CO_2 to CO over Cu-In electrocatalysts: catalyst evolution is the key[J]. ACS Catalysis, 2016, 6(9): 6265-6274.

[51] Ma S, Sadakiyo M, Heima M, et al. Electroreduction of carbon dioxide to hydrocarbons using bimetallic Cu-Pd catalysts with different mixing patterns[J]. Journal of the American Chemical Society, 2017, 139(1): 47-50.

[52] Zhao W G, Yang L N, Yin Y D, et al. Thermodynamic controlled synthesis of intermetallic Au_3Cu alloy nanocrystals from Cu microparticles[J]. Journal of Materials Chemistry A, 2014, 2(4): 902-906.

[53] Kim D, Resasco J, Yu Y, et al. Synergistic geometric and electronic effects for electrochemical reduction of carbon dioxide using gold-copper bimetallic nanoparticles [J]. Nature Communications, 2014, 5: 4948.

[54] Jia F L, Yu X X, Zhang L Z. Enhanced selectivity for the electrochemical reduction of CO_2 to alcohols in aqueous solution with nanostructured Cu-Au alloy as catalyst[J]. Journal of Power Sources, 2014, 252: 85-89.

[55] Lum Y, Kwon Y, Lobaccaro P, et al. Trace levels of copper in carbon materials show significant electrochemical CO_2 reduction activity[J]. ACS Catalysis, 2016, 6(1): 202-209.

[56] Lim D H, Jo J H, Shin D Y, et al. Carbon dioxide conversion into hydrocarbon fuels on defective graphene-supported Cu nanoparticles from first principles[J]. Nanoscale, 2014, 6(10): 5087-5092.

[57] Song Y, Peng R, Hensley D K, et al. High-selectivity electrochemical conversion of CO_2 to ethanol using a copper nanoparticle/N-doped graphene electrode[J]. ChemistrySelect, 2016, 1(19): 6055-6061.

[58] Li Q, Zhu W L, Fu J J, et al. Controlled assembly of Cu nanoparticles on pyridinic-N rich graphene for electrochemical reduction of CO_2 to ethylene[J]. Nano Energy, 2016, 24: 1-9.

[59] Irfan Malik M, Malaibari Z O, Atieh M, et al. Electrochemical reduction of CO_2 to methanol over MWCNTs impregnated with Cu_2O[J]. Chemical Engineering Science, 2016, 152: 468-477.

[60] Safdar Hossain S, Rahman S U, Ahmed S. Electrochemical reduction of carbon dioxide over CNT-supported nanoscale copper electrocatalysts[J]. Journal of Nanomaterials, 2014, 2014: 1-10.

[61] Xie J F, Huang Y X, Li W W, et al. Efficient electrochemical CO_2 reduction on a unique chrysanthemum-like Cu nanoflower electrode and direct observation of carbon deposite[J]. Electrochimica Acta, 2014, 139: 137-144.

[62] Hatsukade T, Kuhl K P, Cave E R, et al. Insights into the electrocatalytic reduction of CO_2 on metallic silver surfaces[J]. Physical Chemistry Chemical Physics, 2014, 16(27): 13814-13819.

[63] Ren D, Deng Y, Handoko A D, et al. Selective electrochemical reduction of carbon dioxide to ethylene and ethanol on copper(I) oxide catalysts[J]. ACS Catalysis, 2015, 5(5): 2814-2821.

[64] Dutta A, Rahaman M, Luedi N C, et al. Morphology matters: tuning the product distribution of CO_2 electroreduction on oxide-derived Cu foam catalysts [J]. ACS Catalysis, 2016, 6(6): 3804-3814.

[65] Verdaguer-Casadevall A, Li C W, Johansson T P, et al. Probing the active surface sites for CO reduction on oxide-derived copper electrocatalysts[J]. Journal of the American Chemical Society, 2015, 137(31): 9808-9811.

[66] Li C W, Ciston J, Kanan M W. Electroreduction of carbon monoxide to liquid fuel on oxide-derived nanocrystalline copper[J]. Nature, 2014, 508(7497): 504-507.

[67] Kas R, Kortlever R, Yılmaz H, et al. Manipulating the hydrocarbon selectivity of copper nanoparticles in CO_2 electroreduction by process conditions[J]. ChemElectroChem, 2014, 2(3): 354-358.

[68] Schouten K J P, Pérez Gallent E, Koper M T M. The influence of pH on the reduction of CO and CO_2 to hydrocarbons on copper electrodes[J]. Journal of Electroanalytical Chemistry, 2014, 716: 53-57.

[69] Mistry H, Varela A S, Bonifacio C S, et al. Highly selective plasma-activated copper catalysts for carbon dioxide reduction to ethylene[J]. Nature Communications, 2016, 7: 12123.

[70] Zhang Y J, Peterson A A. Oxygen-induced changes to selectivity-determining steps in electrocatalytic CO_2 reduc-

tion[J]. Physical Chemistry Chemical Physics, 2015, 17 (6): 4505-4515.

[71] Albo J, Vallejo D, Beobide G, et al. Copper-based metal-organic porous materials for CO_2 electrocatalytic reduction to alcohols[J]. ChemSusChem, 2017, 10(6): 1100-1109.

[72] Kauffman D R, Ohodnicki P R, Kail B W, et al. Selective electrocatalytic activity of ligand stabilized copper oxide nanoparticles[J]. The Journal of Physical Chemistry Letters, 2011, 2(16): 2038-2043.

[73] Verdejo B, Blasco S, González J, et al. CO_2 fixation and activation by CuII complexes of 5,5″-terpyridinophane macrocycles[J]. European Journal of Inorganic Chemistry, 2008, 2008(1): 84-97.

[74] Verdejo B, Aguilar J, García-España E, et al. CO_2 fixation by Cu^{2+} and Zn^{2+} complexes of a terpyridinophane aza receptor. crystal structures of Cu^{2+} complexes, pH-metric, spectroscopic, and electrochemical studies[J]. Inorganic Chemistry, 2006, 45(9): 3803-3815.

[75] Weng Z, Jiang J B, Wu Y S, et al. Electrochemical CO_2 reduction to hydrocarbons on a heterogeneous molecular Cu catalyst in aqueous solution[J]. Journal of the American Chemical Society, 2016, 138(26): 8076-8079.

[76] Hinogami R, Yotsuhashi S, Deguchi M, et al. Electrochemical reduction of carbon dioxide using a copper rubeanate metal organic framework[J]. ECS Electrochemistry Letters, 2012, 1(4): H17-H19.

[77] Senthil Kumar R, Senthil Kumar S, Anbu Kulandainathan M. Highly selective electrochemical reduction of carbon dioxide using Cu based metal organic framework as an electrocatalyst[J]. Electrochemistry Communications, 2012, 25: 70-73.

[78] Lin S, Diercks C S, Zhang Y B, et al. Covalent organic frameworks comprising cobalt porphyrins for catalytic CO_2 reduction in water[J]. Science, 2015, 349(6253): 1208-1213.

[79] Raciti D, Livi K J, Wang C. Highly dense Cu nanowires for low-overpotential CO_2 reduction[J]. Nano Letters, 2015, 15(10): 6829-6835.

[80] Reske R, Duca M, Oezaslan M, et al. Controlling catalytic selectivities during CO_2 electroreduction on thin Cu metal overlayers[J]. The Journal of Physical Chemistry Letters, 2013, 4(15): 2410-2413.

[81] Popic J P, Avramov-Ivic M L, Vukovic N B. Reduction of carbon dioxide on ruthenium oxide and modified ruthenium oxide electrodes in 0.5 M $NaHCO_3$[J]. Journal of Electroanalytical Chemistry, 1997, 421(1): 105-110.

[82] Li J, Prentice G. Electrochemical synthesis of methanol from? CO_2 in high-pressure electrolyte[J]. Journal of The Electrochemical Society, 1997, 144(12): 4284-4288.

[83] H ori Y, Murata A, Takahashi R, et al. Enhanced formation of ethylene and alcohols at ambient temperature and pressure in electrochemical reduction of carbon dioxide at a copper electrode[J]. Journal of the Chemical Society - Chemical Communications, 1988, (1): 17-19.

[84] Kaneco S, Iiba K, Hiei N H, et al. Electrochemical reduction of carbon dioxide to ethylene with high Faradaic efficiency at a Cu electrode in CsOH/methanol[J]. Electrochimica Acta, 1999, 44(26): 4701-4706.

[85] Hori Y, Wakebe H, Tsukamoto T, et al. Adsorption of CO accompanied with simultaneous charge transfer on copper single crystal electrodes related with electrochemical reduction of CO_2 to hydrocarbons[J]. Surface Science, 1995, 335(1/3): 258-263.

电化学二氧化碳还原中的铜基催化剂

杨 帆，邓培林，韩优嘉，潘 静，夏宝玉*

(华中科技大学化学与化工学院，能量转换与存储材料化学教育部重点实验室，
材料化学与服役失效湖北省重点实验室，武汉光电国家研究中心，湖北 武汉 430074)

摘要： 由于不断增加的二氧化碳排放导致全球变暖，且能源短缺等问题日益恶化，将二氧化碳电化学还原为高附加值化学品和燃料引起了极大的兴趣，设计高效催化剂对实现二氧化碳的高效选择性转化具有重要意义. 在所探索的各种催化剂中，铜基催化剂具有良好的开发潜力，可用于烃类生产. 本文综述了铜基电化学二氧化碳转化材料的最新进展. 分别从尺寸结构到不同形式(合金、氧化物)的铜基催化剂，以及分子催化剂等方面展开，重点讨论铜基催化剂上二氧化碳电解还原的反应机理. 最后，对未来高效铜基催化剂的设计提出展望，以促进二氧化碳转化的可持续发展.

关键词： 二氧化碳转化；铜基材料；电催化剂；选择性；反应机理